Supplementary Information (SI) for Journal of Materials Chemistry A.

Supporting Information

Multifunctional Dual Crosslinked $Ti_3C_2T_x$ MXene Based Hydrogels for Wearable Sensors with Enhanced Mechanical Robustness and Broadband Microwave Absorption

Chen Su[a,b,c#], *Mingyu Li*[a#], *Shuai Zhang*[a], *Weiqing Liu*[a], *Yuanzhang Wang*[a], *Peipei Li*[a], *Huanran Feng*[a], *Mingshui Yao*[d], *Weiwei Wu*[a,b,c*], *Lu Zhang*[a,b,c*]

[a]Interdisciplinary Research Center of Smart Sensors, Shaanxi Key Laboratory of High-Orbits-Electron Materials and Protection Technology for Aerospace, School of Advanced Materials and Nanotechnology, Xidian University, Shaanxi, 710126, P.R. China

[b]State Key Laboratory of Electromechanical Integrated Manufacturing of High-performance Electronic Equipments, Xidian University, Shaanxi, 710126, P.R. China

[c]Key Laboratory of Artificial Olfaction of Shaanxi Higher Education Institutes, Xidian University, Shaanxi, 710126, P.R. China

[d]Skate Key Laboratory of Mesoscience and Engineering, Institute of Process Engineering, Chinese Academy of Sciences, Beijing, 100190, P.R. China

*Corresponding authors. E-mail addresses: wwwu@xidian.edu.cn (Weiwei Wu); zhanglu17@xidian.edu.cn (Lu Zhang)

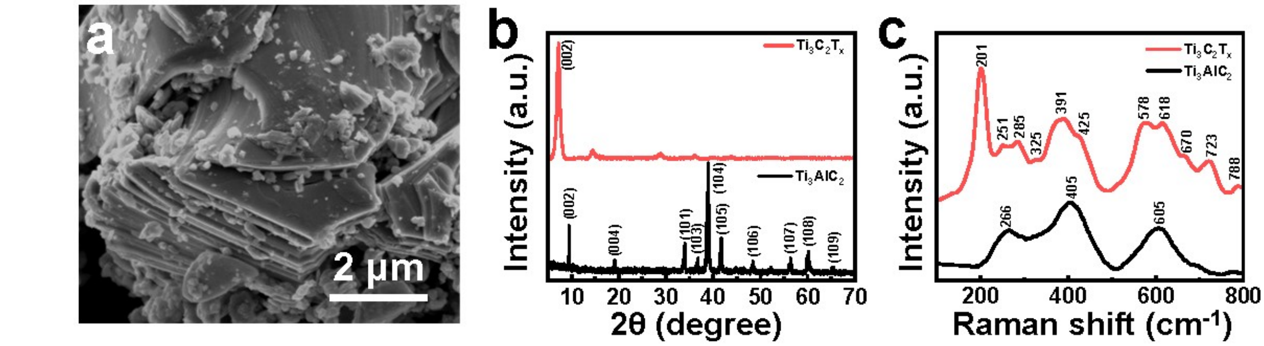

Fig. S1 (a) SEM images of Ti_3AlC_2 MAX phase. (b) XRD patterns of $Ti_3C_2T_x$ MXene and Ti_3AlC_2 MAX phase. (C) Raman spectrum of $Ti_3C_2T_x$ MXene and Ti_3AlC_2 MAX phase.

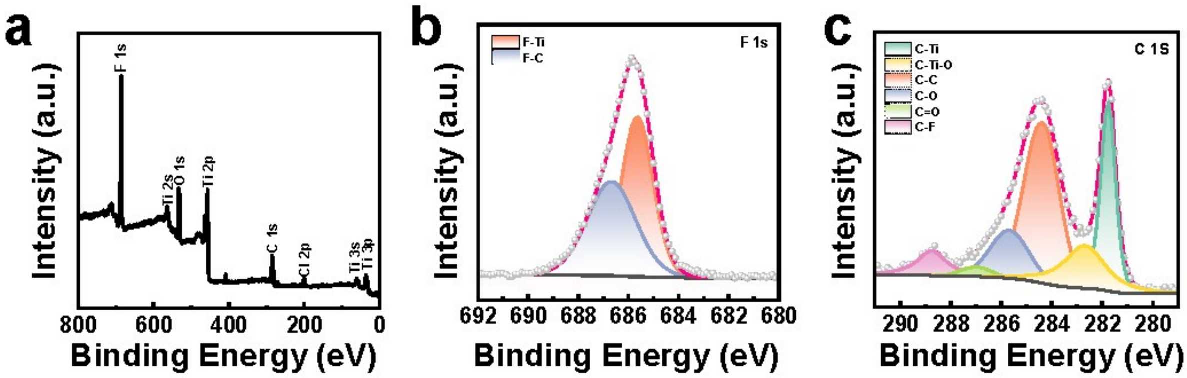

Fig. S2 XPS spectra of (a) full survey scan, (b) F 1s, (c) C 1s for $Ti_3C_2T_x$.

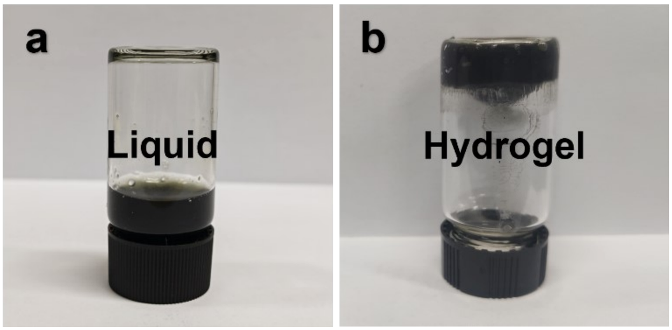

Fig. S3 The optical images of PMP1 hydrogel (a) before and (b) after directional freezing process.

Table S1 The EDS elemental composition table of directional PMP1 hydrogel.

Element	Wt%	At%
Ti	1.31	0.37
C	63.86	72.63
O	28.06	23.96
F	0.42	0.30
S	6.19	2.64
Na	0.17	0.10

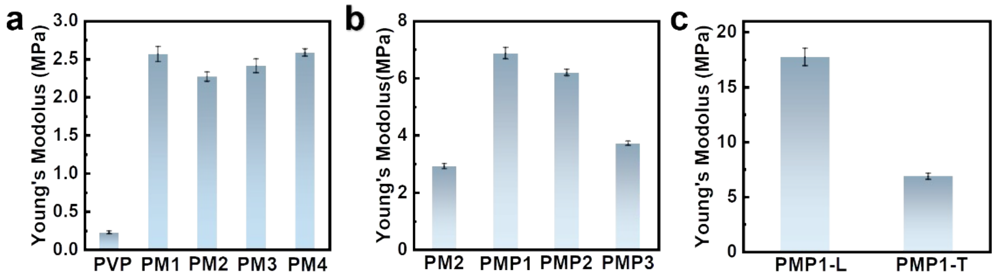

Fig. S4 Calculated Young's modulus for directional frozen hydrogels (a) with different contents of MXene, (b) with different PSS contents, (c) under transverse and longitudinal stress.

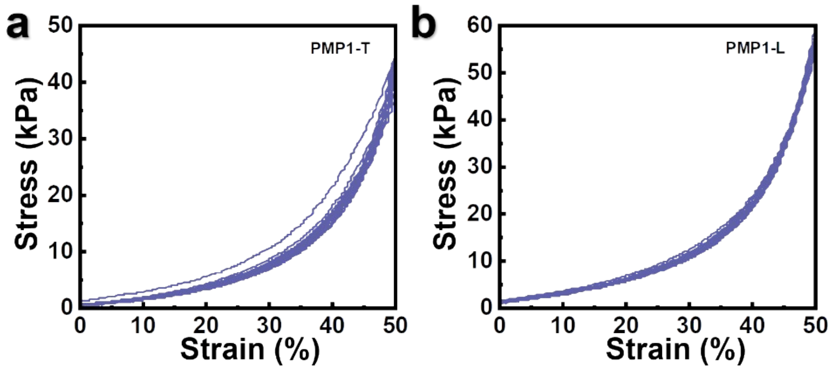

Fig. S5 Compressive stress-strain curves of directional PMP1 hydrogel in the (a) transverse and (b) longitudinal directions.

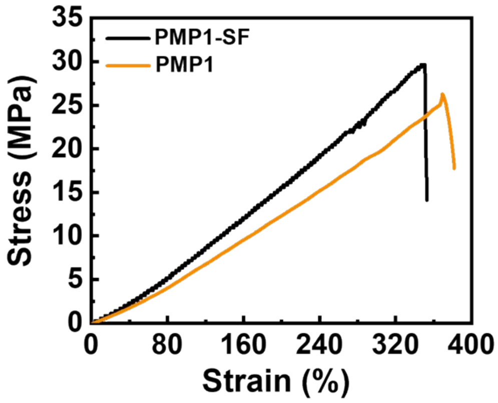

Fig. S6 Comparative mechanical performance of PMP1 and PMP1-SF hydrogels. Tensile stress–strain curves demonstrate that PMP1-SF exhibits a slightly higher Young's modulus than PMP1.

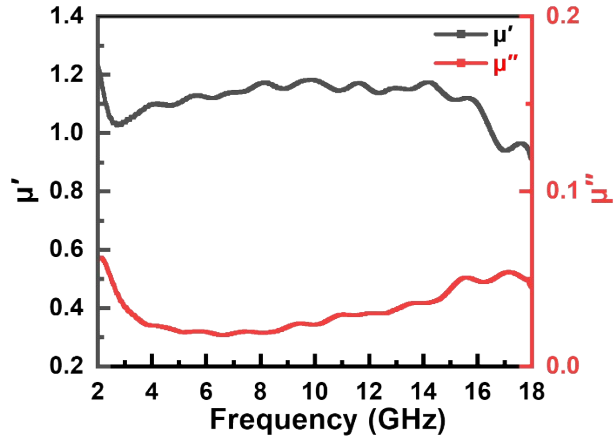

Fig. S7 Frequency-dependent complex permeability characteristics of the directional PMP1-SF hydrogel. The real part of permeability (μ') remains nearly 1.0 over the 2–18 GHz frequency range, while (b) the imaginary part (μ'') is close to 0.0, indicating negligible magnetic loss.

Table S2 Microwave absorption performance of $Ti_3C_2T_x$ MXene-based microwave absorption materials

Materials	RL_{min} (dB)	EAB (RL≤−10 dB)		Refs.
		Value (GHz)	d (mm)	
$Ti_3C_2T_x$ MXenes	-27.5@17.10 GHz @4.00 mm	3.00	2.00	[1]
MXene/PI arrogel	-45.4@9.59 GHz @3.00 mm	5.10	2.00	[2]
MXene/PEO aerogel	-50.8@6.72 GHz @1.70 mm	5.20	1.70	[3]
Anisotropic MXene/polyimide aerogel	-41.8@6.00 GHz @4.00 mm	6.50	1.91	[4]
$Ti_3C_2T_x$/PPy	-49.2@8.50 GHz @3.20 mm	4.90	3.20	[5]
MXene/MoS_2 heterostructure	-46.72@4.32 GHz @2.00 mm	4.32	2.00	[6]
porous MXene/CNTs microspheres	-45 dB@10.00 GHz @2.70 mm	4.90	1.90	[7]
MXene/CNTs/PI aerogel	-50.03@13.70 GHZ @1.80mm	5.60	1.80	[8]
MXene@RGO aerogel	-31.2@8.00 GHz @3.05 mm	5.40	2.05	[9]
Directional PVA/$Ti_3C_2T_x$/PSS hydrogels	**-55.5@10.73 GHz @2.50 mm**	**6.34**	**2.00**	**This work**

References

[1] G. Cui, X. Sun, G. Zhang, Z. Zhang, H. Liu, J. Gu, G. Gu, Electromagnetic absorption performance of two-dimensional MXene $Ti_3C_2T_x$ exfoliated by HCl + LiF etchant with diverse etching times, Mater. Lett. 252 (2019) 8-10.

[2] J. Liu, H.B. Zhang, X. Xie, R. Yang, Z. Liu, Y. Liu, Z.Z. Yu, Multifunctional, Superelastic, and Lightweight MXene/Polyimide Aerogels, Small 14(45) (2018) e1802479.

[3] X. Zhou, S. Li, M. Zhang, X. Yuan, J. Wen, H. Xi, H. Wu, X. Ma, MXene/PEO aerogels with two-hierarchically porous architecture for electromagnetic wave absorption, Carbon 204 (2023) 538-546.

[4] Y. Dai, X. Wu, Z. Liu, H.-B. Zhang, Z.-Z. Yu, Highly sensitive, robust and anisotropic MXene aerogels for efficient broadband microwave absorption, Composites, Part B 200 (2020) 108263.

[5] Y. Tong, M. He, Y. Zhou, X. Zhong, L. Fan, T. Huang, Q. Liao, Y. Wang, Hybridizing polypyrrole chains with laminated and two-dimensional $Ti_3C_2T_x$ toward high-performance electromagnetic wave absorption, Appl. Surf. Sci. 434 (2018) 283-293.

[6] X. Li, C. Wen, L. Yang, R. Zhang, Y. Li, R. Che, Enhanced visualizing charge distribution of 2D/2D MXene/MoS_2 heterostructure for excellent microwave absorption performance, J. Alloys Compd. 869

(2021) 159365.
[7] Y. Cui, F. Wu, J. Wang, Y. Wang, T. Shah, P. Liu, Q. Zhang, B. Zhang, Three dimensional porous MXene/CNTs microspheres: Preparation, characterization and microwave absorbing properties, Composites, Part A 145 (2021) 106378.
[8] Y. Cui, K. Yang, F. Zhang, Y. Lyu, Q. Zhang, B. Zhang, Ultra-light MXene/CNTs/PI aerogel with neat arrangement for electromagnetic wave absorption and photothermal conversion, Composites, Part A 158 (2022) 106986.
[9] L. Wang, H. Liu, X. Lv, G. Cui, G. Gu, Facile synthesis 3D porous MXene $Ti_3C_2T_x$@RGO composite aerogel with excellent dielectric loss and electromagnetic wave absorption, J. Alloys Compd. 828 (2020) 154251.